the plant journal

SEB Society for Experimental Biology

*The Plant Journal* (2016) **85,** 410–423 doi: 10.1111/tpj.13114

# Trehalose 6–phosphate coordinates organic and amino acid metabolism with carbon availability

**Carlos M. Figueroa[1], Regina Feil[1], Hirofumi Ishihara[1], Mutsumi Watanabe[1], Katharina Kölling[2], Ursula Krause[1], Melanie Höhne[1], Beatrice Encke[1], William C. Plaxton[3], Samuel C. Zeeman[2], Zhi Li[4], Waltraud X. Schulze[4], Rainer Hoefgen[1], Mark Stitt[1] and John E. Lunn[1,*]**

[1]*Max Planck Institute of Molecular Plant Physiology, Potsdam-Golm 14476, Germany,*

[2]*Department of Biology, Institute of Agricultural Sciences, ETH Zurich, Zurich 8092, Switzerland,*

[3]*Department of Biology and Department of Biomedical and Molecular Sciences, Queen's University, Kingston, Ontario, K7L 3N6, Canada, and*

[4]*Department of Plant Systems Biology, University of Hohenheim, Stuttgart 70593, Germany*

Received 14 October 2015; revised 14 December 2015; accepted 21 December 2015; published online 30 December 2015.
*For correspondence (email lunn@mpimp-golm.mpg.de).

## SUMMARY

**Trehalose 6–phosphate (Tre6P) is an essential signal metabolite in plants, linking growth and development to carbon metabolism. The sucrose–Tre6P nexus model postulates that Tre6P acts as both a signal and negative feedback regulator of sucrose levels. To test this model, short-term metabolic responses to induced increases in Tre6P levels were investigated in *Arabidopsis thaliana* plants expressing the *Escherichia coli* Tre6P synthase gene (*otsA*) under the control of an ethanol-inducible promoter. Increased Tre6P levels led to a transient decrease in sucrose content, post-translational activation of nitrate reductase and phosphoenolpyruvate carboxylase, and increased levels of organic and amino acids. Radio-isotope ($^{14}CO_2$) and stable isotope ($^{13}CO_2$) labelling experiments showed no change in the rates of photoassimilate export in plants with elevated Tre6P, but increased labelling of organic acids. We conclude that high Tre6P levels decrease sucrose levels by stimulating nitrate assimilation and anaplerotic synthesis of organic acids, thereby diverting photoassimilates away from sucrose to generate carbon skeletons and fixed nitrogen for amino acid synthesis. These results are consistent with the sucrose–Tre6P nexus model, and implicate Tre6P in coordinating carbon and nitrogen metabolism in plants.**

**Keywords: *Arabidopsis thaliana* [L.] Heynh., nitrate reductase, protein phosphorylation, phosphoenolpyruvate carboxylase, sucrose, trehalose-6–phosphate synthase, ubiquitination.**

## INTRODUCTION

Trehalose 6–phosphate (Tre6P), the intermediate of trehalose biosynthesis, is an essential signal metabolite that links the growth and development of plants to their metabolic status (Lunn *et al.*, 2014). Tre6P is synthesized from UDP-glucose (UDPGlc) and glucose 6–phosphate (Glc6P) by Tre6P synthase (TPS, EC 2.4.1.15), and dephosphorylated to trehalose by Tre6P phosphatase (TPP, EC 3.1.3.12) (Cabib and Leloir, 1958). In *Arabidopsis thaliana*, loss of AtTPS1, the predominant catalytically active TPS isoform (Delorge *et al.*, 2015), leads to embryo arrest, stunted vegetative growth and delayed flowering (Eastmond *et al.*, 2002; van Dijken *et al.*, 2004; Gomez *et al.*, 2006, 2010; Wahl *et al.*, 2013). Constitutive over-expression of the *Escherichia coli* TPS in *A. thaliana* (*35S:otsA*) plants gives rise to plants with small leaves, precocious flowering and increased shoot branching, whereas over-expression of the *E. coli* TPP (*35S:otsB*) has opposite effects, implicating Tre6P as the trigger for these developmental phenotypes (Schluepmann *et al.*, 2003; Yadav *et al.*, 2014).

Tre6P levels are extremely low in carbon-starved *A. thaliana* seedlings, increase more than 25-fold after sucrose addition, and are more strongly correlated with sucrose than with glucose, fructose or related metabolites (Lunn *et al.*, 2006). Diurnal fluctuations in Tre6P and sucrose are also highly correlated in rosette leaves of soil-grown plants (Lunn *et al.*, 2006). Together, these observations led to the proposal that Tre6P acts as a signal of sucrose availability (Lunn *et al.*, 2006). The close relationship between sucrose and Tre6P levels has been confirmed by subsequent studies in *A. thaliana* (Wingler *et al.*, 2012;

Carillo *et al.*, 2013; Martins *et al.*, 2013; Nunes *et al.*, 2013a; Wahl *et al.*, 2013; Sulpice *et al.*, 2014; Yadav *et al.*, 2014) and other species (Debast *et al.*, 2011; Martinez-Barajas *et al.*, 2011). Strong correlations between Tre6P and sucrose were also seen in *35S:otsA* and *35S:otsB A. thaliana* plants, although the ratios of Tre6P to sucrose were higher and lower than in wild-type plants, respectively (Yadav *et al.*, 2014). This led to proposal of the sucrose–Tre6P nexus model, which postulates that Tre6P acts as both a signal and negative feedback regulator of sucrose levels, thereby helping to maintain intracellular sucrose concentrations within a range that is optimal for the cell (Yadav *et al.*, 2014). As part of the nexus model, it is envisaged that the set point and dynamic range of the sucrose–Tre6P nexus vary according to the specific requirements of various tissue and cell types at various developmental stages (Lunn *et al.*, 2014), and there is evidence that the sucrose–Tre6P relationship is also adjusted in response to changes in environmental conditions, e.g. low temperature (Carillo *et al.*, 2013).

Given the central role of sucrose in plant metabolism (Lunn, 2008), and its widespread influence on gene and protein expression at the transcriptional, translational and post-translational levels (Lastdrager *et al.*, 2014), the sucrose–Tre6P nexus model may explain why perturbation of Tre6P levels has such profound effects on plant growth and development. However, little is known of the molecular mechanisms that link sucrose and Tre6P, and these are difficult to investigate in *tps* null mutants or the constitutive *35S:otsA* and *35S:otsB* lines due to their highly pleiotropic phenotypes.

Using ethanol-inducible otsA lines, Martins *et al.* (2013) found that high night-time levels of Tre6P inhibit starch breakdown in *A. thaliana* leaves, thereby limiting the rate of sucrose synthesis at night and decreasing sucrose to very low levels. Tre6P may also influence sucrose levels by stimulating consumption of sucrose for growth. In young developing tissues, inhibition of the sucrose-non-fermenting 1-related protein kinase (SnRK1) by Tre6P may play a role in stimulating sucrose consumption (Zhang *et al.*, 2009).

To better understand the nexus between Tre6P and sucrose, we used one of the ethanol-inducible otsA lines (TPS29.2) established by Martins *et al.* (2013) to investigate metabolic responses to short-term increases in Tre6P in the daytime, when the decrease in sucrose may be less extreme. After induction of otsA expression, increasing levels of Tre6P were accompanied by a small decrease in sucrose content, while the levels of several organic and amino acids increased. The molecular mechanisms underlying these metabolite changes were investigated by $^{13}CO_2$ and $^{14}CO_2$ labelling experiments, revealing the influence of Tre6P on post-translational regulation of key enzymes involved in nitrate assimilation and provision of precursors for amino acid synthesis.

## RESULTS

### Effects of TPS induction on sucrose and starch metabolism

All of the experiments reported here were performed using the ethanol-inducible TPS29.2 line and the AlcR line expressing only the ethanol-binding transcription factor, as described by Martins *et al.* (2013). Plants were grown under equinoctial conditions (12 h light/12 h dark) or long-day conditions (16 h light/8 h dark), and 4- or 3-week-old plants, respectively, were sprayed with either water (non-induced) or ethanol (induced) at the start of the light period (i.e. ZT0, where ZT or zeitgeber time refers to the number of hours after the preceding dawn). Samples were harvested every 2 h until the end of the day for metabolite and enzyme analysis. The results of both diurnal cycle experiments were qualitatively very similar. However, as some of the more transient metabolic responses were most evident under long-day conditions, we focus on those experiments (Figure 1 and Figure S1). Plants grown under a 12 h photoperiod were marginally carbon-limited, while plants grown under long-day conditions (16 h photoperiod) were carbon-replete (Sulpice *et al.*, 2014), which may account for the quantitative differences in their responses to induced increases in Tre6P. The data from the 12 h photoperiod experiment are shown in Figure S2. Two methods of statistical analysis were used. In Figure 1 and Figures S1 and S2, asterisks indicate values from the induced TPS29.2 plants that were significantly different from all three of the controls (i.e. water- and ethanol-treated AlcR and non-induced TPS29.2) at that time point, according to a one-way analysis of variance (ANOVA) with Holm–Šídák post hoc testing. As a more sensitive test for weaker but consistent trends across multiple time points, we also analysed the data using one-way repeated-measures ANOVA. Metabolites that were found to be significantly increased or decreased in the induced TPS29.2 plants by this statistical test are shown in blue and red, respectively, on a map of central metabolism (Figure 2 and Figure S3). The *P* values from repeated-measures ANOVA of the 16 and 12 h photoperiod experiments are given in Tables S1 and S2, respectively.

Tre6P increased during the day under the three control treatments, presumably reflecting the parallel increase in sucrose levels (see also Lunn *et al.*, 2006). From 4-6 h after induction, the levels of Tre6P in the induced TPS29.2 plants were significantly higher than in the three controls (Figure 1a,b), as previously observed by Martins *et al.* (2013). In the 12 h photoperiod experiment, Tre6P was already significantly higher in the induced TPS29.2 plants by 4 h after induction (Figure S2a). In both experiments, increasing Tre6P levels in the induced plants were accompanied by a transient 20–30% decrease in sucrose content (Figure 1b and Figure S2a). There was only a slight, and usually

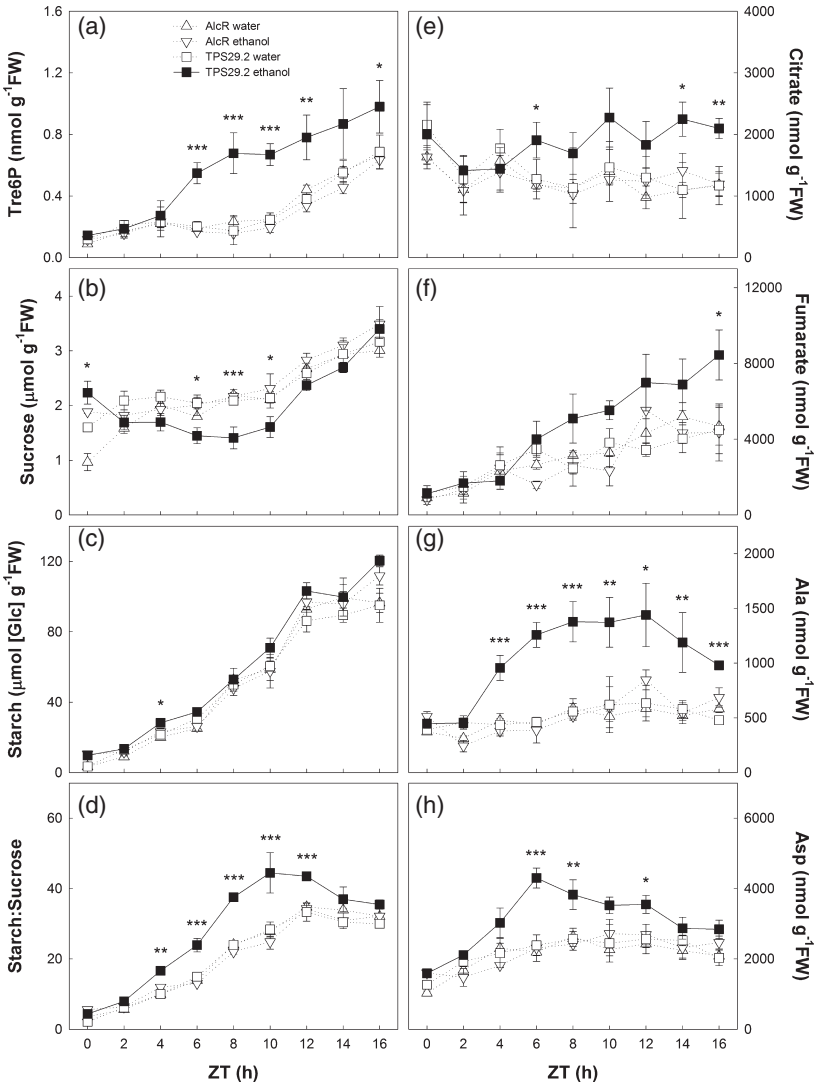


**Figure 1.** Changes in metabolites after induction of TPS over-expression.
Three-week-old TPS29.2 and AlcR plants, grown under long-day conditions (16 h photoperiod) were sprayed with water or 2% v/v ethanol at dawn (ZT0), and samples were harvested every 2 h for metabolite analysis. Values are means ±SD ($n = 3$). Asterisks indicate statistically significant differences between the induced TPS29.2 and control samples: $*P < 0.05$, $**P < 0.01$ and $***P < 0.001$ (one-way ANOVA, Holm–Šídák post hoc testing). ZT, Zeitgeber time (hours after dawn).

non-significant, increase in starch in the induced plants compared to the controls. The ratio of starch to sucrose was significantly higher, due mainly to the lower sucrose content in the induced plants (Figures 1c,d and 2, and Figures S2a and S3). Glucose and fructose were slightly elevated in the induced plants, especially around the middle of the day (ZT8) in the long-day experiment (Figures S1a and S2a). There were no obvious changes in the maximal catalytic activities of acid or neutral invertases (Figure S2e).

Among the intermediates of sucrose biosynthesis, fructose 6–phosphate (Fru6P) and sucrose 6′–phosphate (Suc6P) were slightly lower in the induced plants in the long-day experiment (Figure 2, and Figures S1a and S2a), but UDPGlc was not significantly different from the controls in either experiment. The levels of other hexose phosphates, including Glc6P, which is an allosteric activator of sucrose-phosphate synthase (SPS), fructose 1,6–bisphosphate, glucose 1–phosphate, mannose 6–phosphate and galactose 1–phosphate, were also significantly lower in the induced plants (Figure 2 and Table S1). Levels of fructose 2,6-bisphosphate (Fru2,6BP) increased during the day in the controls, following the increase in sucrose as previously seen (Stitt, 1990a). However, there were no significant differences between induced and control plants in the levels of Fru2,6BP (Figure S2a) or the maximal and selective activities of SPS (Figure S2e).

### Effects of TPS induction on respiratory intermediates and amino acids

Induction of TPS had no significant effect on phosphoenolpyruvate (PEP) or pyruvate, although the ratio of PEP to pyruvate was significantly lower at ZT8 in the 12 h photoperiod experiment (Figures S1b and S2b). In the long-day experiment, the induced TPS29.2 plants had higher levels of citrate and fumarate, with the greatest

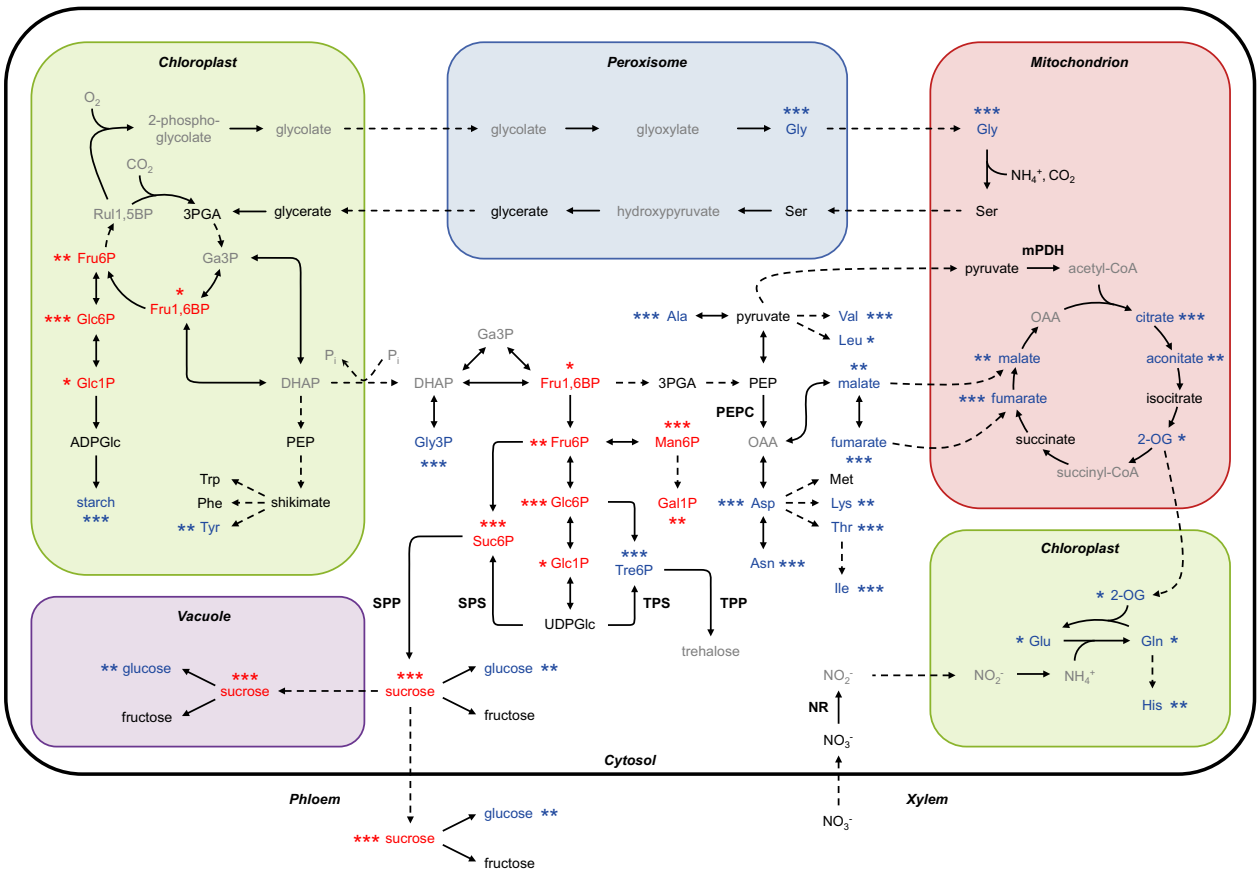


**Figure 2.** Overview of metabolite changes after induction of TPS expression.
Metabolite data from the experiment described in Figure 1 are displayed on a map of central metabolism. Solid arrows represent single-enzyme reactions and dashed arrows represent multiple reactions or transport between compartments. Data were analysed by one-way repeated-measures ANOVA with Holm–Šídák post hoc testing (see Table S1). Asterisks indicate statistically significant differences between the induced TPS29.2 and control sample: $*P < 0.05$, $**P < 0.01$ and $***P < 0.001$. Colours indicate which metabolites were significantly increased (blue) or decreased (red), or unchanged (black). Metabolites shown in grey were not measured.

differences towards the end of the day, while the level of 2–oxoglutarate (2–OG) was higher around the middle of the day (Figure 1e,f and Figure S1c). The repeated-measures ANOVA additionally revealed that aconitate and malate levels were likely to be higher in the induced TPS29.2 plants (Figure 2 and Table S1), although there were no significant differences between induced and control plants at any individual time point (Figure S1c). The induced TPS29.2 plants in the 12 h photoperiod experiment showed no differences in citrate content, but did have elevated levels of 2–OG, fumarate and malate (Figures S2c and S3).

Even stronger responses to elevated Tre6P were observed for several amino acids. Within 4-6 h of induction in both experiments, the induced TPS29.2 plants showed significantly increased levels of Ala and Asp (Figure 1g,h and Figure S2d). There were also significantly higher levels of Val, Asn, Thr, Lys and Ile in the induced TPS29.2 plants (Figure 2 and Figure S1d), and a particularly marked increase in Gly (Figure S1d and S2d). Ser showed a tendency to be decreased in the induced TPS29.2 plants in the 12 h photoperiod experiment, but not under long-day conditions (Figure 2, and Figures S1d, S2d and S3). Neither Glu nor Gln was significantly altered in the induced TPS29.2 plants compared to the controls at any time point, but overall there was a significant trend towards higher Glu and Gln levels in the induced plants (Figure 2 and Figure S1d). The total amino acid content of the induced TPS29.2 plants was higher than in the control plants when grown under a 16 h photoperiod (Figure S1d), but was not significantly different from the controls in the 12 h photoperiod experiment (Figure S2d).

Under long-day conditions, the total amount of carbon in tricarboxylic acid (TCA) pathway intermediates and amino acids was higher in the induced TPS29.2 plants than the controls from ZT6 until the end of the photoperiod (Figure S4a). The differences between the induced TPS29.2 and control plants were smaller when soluble sugars (sucrose, glucose and fructose) were included in the calculation (Figure S4b), and almost disappeared (significant

difference only at ZT6) when starch was also included (Figure S4c). These comparisons suggest there was only a minor increase, if any, in the net carbon assimilation rate in the induced TPS29.2 plants, and that the increased amounts of carbon in the TCA pathway intermediates, amino acids and hexoses were largely offset by the decrease in the pool of carbon in sucrose (Figure 1b). There were a few very minor differences between the induced TPS29.2 and control plants in terms of their carbon pool sizes when grown under a 12 h photoperiod (Figure S4d–f), indicating that the increases in some individual organic and amino acids were completely offset by the decrease in sucrose (Figure S2a).

**TPS induction alters photoassimilate partitioning into sucrose and organic acids**

The metabolic responses to increasing Tre6P levels were investigated further by single-leaf $^{14}C$-labelling experiments (Kölling *et al.*, 2013) using induced TPS29.2 and control plants. Plants grown under long-day conditions were induced at ZT1, and leaf 4 was supplied with $^{14}CO_2$ as a 5 min pulse at ZT7 and ZT13 (i.e. 6 and 12 h after induction), then returned to $^{12}CO_2$ for a 1 h chase period before harvesting. The distribution of label was analysed separately in leaf 4 and the rest of the rosette. In leaf 4 from the induced TPS29.2 plants (labelled at ZT13), there was significantly less $^{14}C$ in the neutral fraction (containing soluble sugars) and more in the acidic fraction (containing organic acids and phosphorylated intermediates) than in the control plants, but no difference in the labelling of the basic fraction (containing amino acids) (Figure S5a–c). Similar but not statistically significant trends were observed after pulse labelling at ZT7. There were no significant differences between the induced TPS29.2 and control plants in terms of incorporation of the label into starch, or in the amount of label exported from leaf 4 to the rest of the rosette (Figure S5d,e).

**TPS induction promotes carbon flux into organic acids**

The elevated organic acid levels of the induced TPS29.2 plants and the $^{14}C$-labelling results suggested that the decrease in sucrose triggered by increasing Tre6P levels was mainly due to increased flux of carbon into respiratory pathways. To test this hypothesis, TPS29.2 plants grown under long-day conditions were induced at ZT0, and whole rosettes of induced and control plants were pulse-labelled with $^{13}CO_2$ from ZT4 to ZT10, at which time Tre6P was expected to be significantly increased in the induced TPS29.2 plants. Samples were taken at ZT4 (before the pulse) and at ZT6, ZT8 and ZT10 for analysis of organic acid isotopomers by LC-MS/MS.

Tre6P levels were very similar to those observed in previous experiments, with Tre6P levels in the induced TPS29.2 plants increasing significantly above the controls from 6 h after induction (Figure S6a). The amounts of TCA pathway intermediates were also similar to previous experiments, with the induced plants having higher 2–OG and fumarate levels than the controls (Figure S6b–h). There was substantial $^{13}C$ enrichment of Tre6P in all of the plants (>80% at ZT10; Figure 3a). Although there were no significant differences between the induced TPS29.2 and control plants in terms of $^{13}C$ enrichment of Tre6P, the total amount of Tre6P (and thus the total amount of $^{13}C$ in Tre6P) was clearly higher in the induced TPS29.2 plants (Figure S6a), which is consistent with increased flux of $^{13}C$ into Tre6P in the induced plants. The $^{13}C$ enrichment of most of the measured organic acids, including citrate, aconitate, isocitrate, 2–OG, malate and fumarate, was significantly higher in the induced TPS29.2 plants than in the controls (Figure 3b–h). The only exception was succinate, which showed no significant differences between induced and control plants (Figure 3f). The increases in $^{13}C$ enrichment (Figure 3) were greater than the increases in the total amounts of organic acids (Figure S6), reflecting the sensitivity of $^{13}C$ enrichment as an indicator of flux changes in the metabolically active pools (Szecowka *et al.*, 2013).

**TPS induction leads to post-translational activation of PEP carboxylase and nitrate reductase**

PEP carboxylase (PEPC) catalyses the anaplerotic conversion of PEP and bicarbonate ($HCO_3^-$) into oxaloacetate (OAA) in the cytosol, which may subsequently be transaminated to Asp, reduced to malate or fumarate, or fed directly into the TCA pathway in the mitochondria to generate other organic acids (Plaxton and Podestá, 2006). The increased flux of $^{13}C$ into organic acids in the induced TPS29.2 plants suggested that PEPC may have been activated. PEPC activity is regulated by multiple mechanisms, including protein phosphorylation and mono-ubiquitination, which activate and deactivate the enzyme, respectively, by affecting the sensitivity to inhibition by malate (Hartwell *et al.*, 1999; O'Leary *et al.*, 2011b). We analysed the activation status of PEPC in induced TPS29.2 and control plants by immunoblotting of samples harvested at 6 h after induction. This was the time at which we observed some of the earliest statistically significant effects on metabolite levels in previous experiments, presumably reflecting primary responses to increased Tre6P.

We first used a polyclonal antibody raised against the castor bean (*Ricinus communis*) PPC3 isoform of PEPC (anti-RcPPC3), which recognizes two PEPC proteins in *A. thaliana* leaf extracts: a 107 kDa protein corresponding to a non-ubiquitinated plant-type PEPC polypeptide (p107), and a 110 kDa protein corresponding to a mono-ubiquitinated polypeptide (p110) (O'Leary *et al.*, 2011a). In castor bean, comparable p107 and p110 PEPC proteins were shown by peptide mass spectrometry to be derived from the same *RcPEPC* gene (Uhrig *et al.*, 2008). Likewise, the

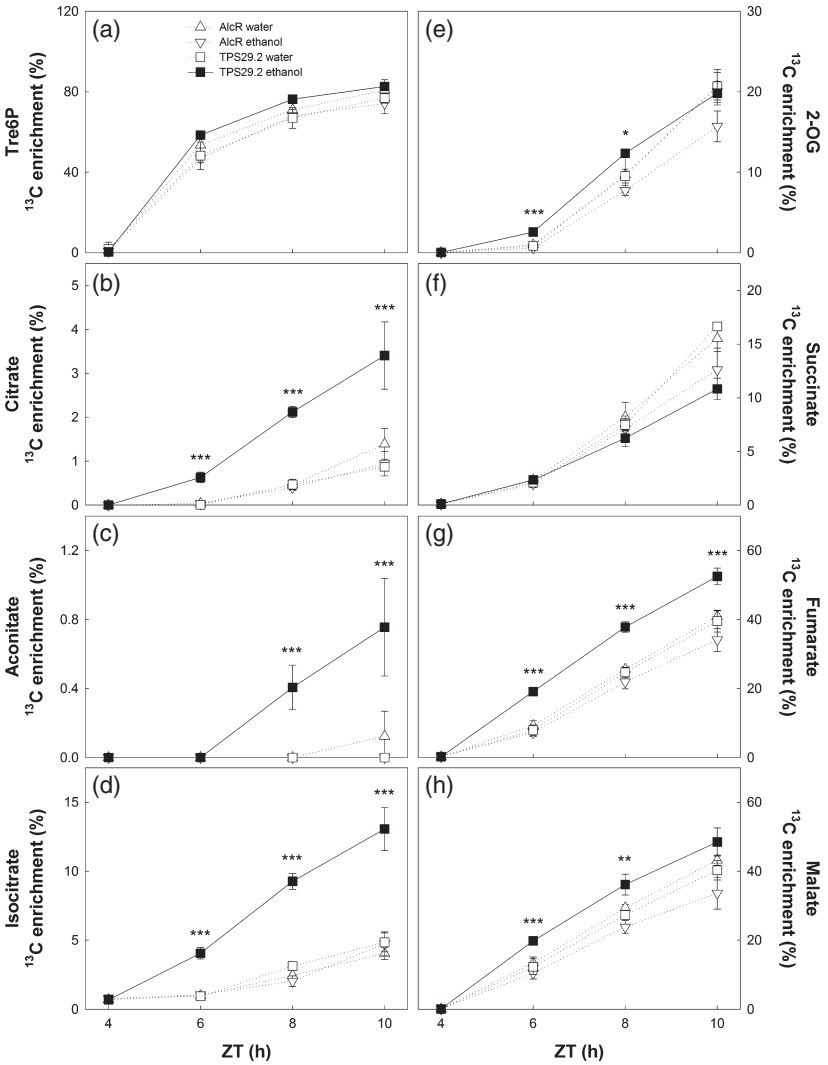


**Figure 3.** Effect of TPS induction on carbon fluxes into Tre6P and organic acids.
Three-week-old TPS29.2 and AlcR plants, grown under long-day conditions (16 h photoperiod) were sprayed with water or 2% v/v ethanol at dawn (ZT0) and supplied with $^{13}CO_2$ from ZT4 to ZT10. Isotopomers were measured by LC-MS/MS to determine $^{13}$C enrichment. Values are means ±SD ($n$ = 4). Asterisks indicate statistically significant differences between the induced TPS29.2 and control samples: $*P < 0.05$, $**P < 0.01$ and $***P < 0.001$ (one-way ANOVA, Holm–Šídák post hoc testing). ZT, Zeitgeber time (hours after dawn).

p107 and p110 proteins in harsh hakea (*Hakea prostrata*) and sorghum (*Sorghum bicolor*) were confirmed to have single-gene origin from the corresponding *HpPEPC* and *SbPEPC* genes (Shane *et al.*, 2013; Ruiz-Ballesta *et al.*, 2014), suggesting that a similar relationship may exist for the p107 and p110 PEPC proteins in *A. thaliana*. The percentage of p110 was approximately 40% lower in the induced TPS29.2 plants than in the controls (Figure 4a). Immunoblotting with an anti-pSer11 polyclonal antibody, which recognizes the activated phospho-Ser11 form of plant-type PEPC (Gregory *et al.*, 2009), revealed the presence of phosphorylated p107 subunits in the positive control plants (Pi-starved seedlings) and induced TPS29.2 plants, but not in the negative controls (Figure 4b). Phosphorylated and non-phosphorylated forms of PEPC were resolved by electrophoresis in polyacrylamide gels containing Phos-tag reagent, which retards the migration of phosphorylated proteins (Kinoshita *et al.*, 2006). Immunoblotting with the anti-RcPPC3 antibody revealed the presence of an immunoreactive protein with an apparent molecular mass of approximately 140 kDa in the induced TPS29.2 samples but not in the control samples, while two of the smaller polypeptides were absent or greatly decreased in the induced TPS29.2 samples (Figure S7). These results indicate a shift from the deactivated (non-phosphorylated and mono-ubiquitinated) form of PEPC to the activated (phosphorylated and non-ubiquitinated) form in induced TPS29.2 plants.

In addition to the carbon skeletons provided by the respiratory and anaplerotic pathways, amino acid synthesis also requires a source of reduced nitrogen. Therefore, we investigated whether there was any change in the activity of nitrate reductase (NR), which catalyses the first step in nitrate assimilation and is a regulatory enzyme in this pathway. The maximal catalytic activity of NR ($V_{max}$) was similar for all lines and treatments, but the selective activity ($V_{sel}$), measured in an assay (Kaiser and Huber, 2001) that favours the activated (non-phosphorylated) form of the

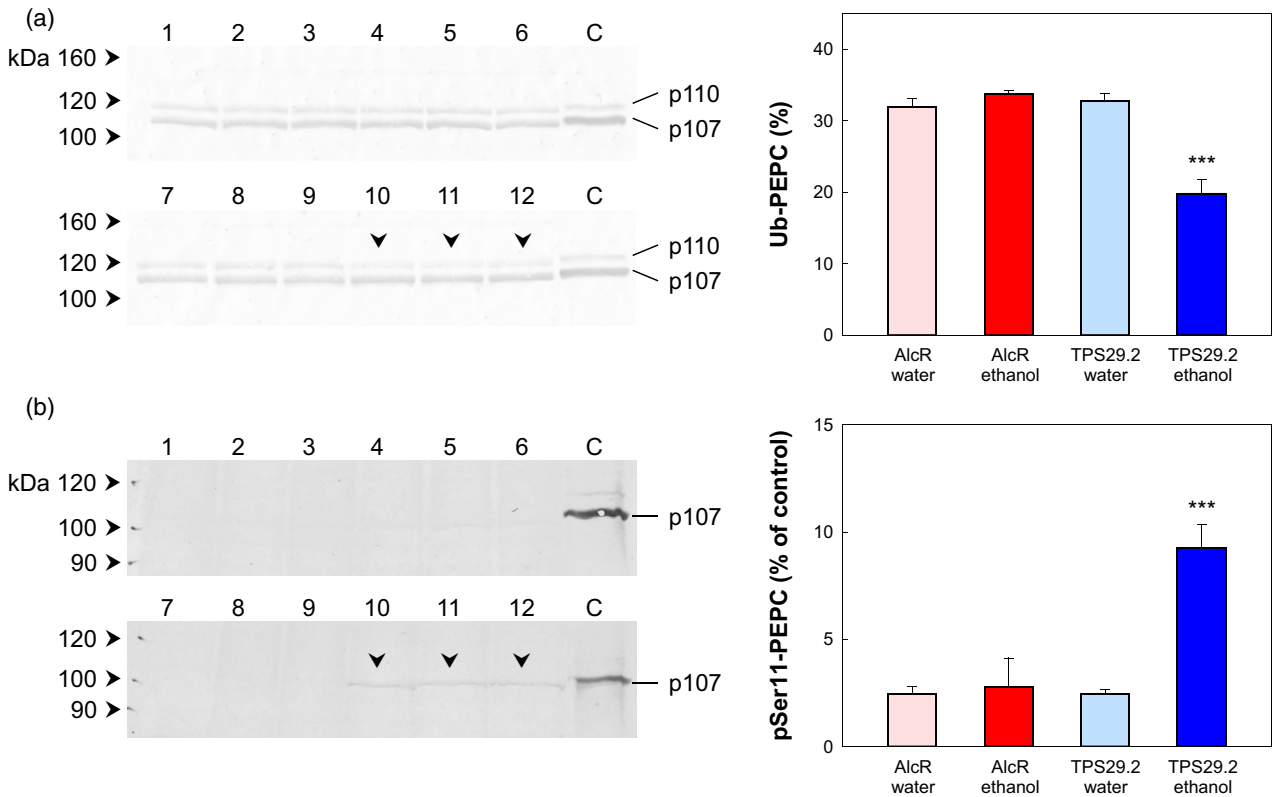


**Figure 4.** TPS induction leads to post-translational modifications of PEPC.
Three-week-old TPS29.2 and AlcR plants, grown under long-day conditions (16 h photoperiod), were sprayed with water or 2% v/v ethanol at dawn (ZT0) and harvested at ZT6.
(a) Anti-RcPPC3 immunoblot showing the mono-ubiquitinated (p110) and non-ubiquitinated (p107) forms of PEPC. The histogram shows the fraction of mono-ubiquitinated PEPC expressed as a percentage of total PEPC.
(b) Anti-pSer11 immunoblot showing the phosphorylated form of PEPC (p107). The histogram shows the abundance of the phosphorylated form of PEPC expressed as a percentage of the control (Pi-starved *A. thaliana* seedlings).
Lanes 1–3, AlcR (water); lanes 4–6, AlcR (ethanol); lanes 7–9, TPS29.2 (water); lanes 10–12, TPS29.2 (ethanol); lane C, control. Values are means ± SD ($n = 3$), and the significant difference between the induced TPS29.2 and control samples is indicated by asterisks: ***$P < 0.001$ (one-way ANOVA, Holm–Šídák post hoc testing). ZT, Zeitgeber time (hours after dawn).

enzyme, was significantly higher in the induced TPS29.2 plants (Figure 5). Very similar changes were seen in samples from the 12 h photoperiod experiment (Figure S2e).

Protein samples from plants grown under equinoctial conditions and harvested at 6 h after induction were subjected to phosphopeptide enrichment and analysed by mass spectrometry. The normalized ion intensity for the (oxM)A(pS$^{11}$)IDAQLR phosphopeptide from the predominant PEPC isoform in leaves (PPC2; At2g42600) (Shi *et al.*, 2015) was approximately twofold higher in the induced TPS29.2 plants than in the controls (Figure 6a), whereas total PPC2 peptide abundance was similar in all samples (Figure 6b). The SV(pS$^{534}$)TPFMNTTAK phosphopeptide, derived from the most abundant NR isoform in leaves (NIA2, At1g37130) (Wilkinson and Crawford, 1991), was found in all three of the controls, with similar normalized ion intensities, but not in the induced TPS29.2 samples (Figure 6c). The total NIA2 peptide abundance did not differ significantly between the induced and control plants (Figure 6d). Representative spectra for the analysed phosphopeptides are shown in Figure S8.

## DISCUSSION

### Higher Tre6P triggers a decrease in sucrose levels

The ethanol-inducible otsA lines established by Martins *et al.* (2013) enabled us to investigate the short-term metabolic responses to increases in Tre6P in plants that are essentially wild-type in character before induction. Significant increases in Tre6P were seen within 4–6 h of induction (Figure 1a and Figure S2a), as reported by Martins *et al.* (2013).

In both the long-day and equinoctial photoperiod experiments, sucrose was among the first of the measured metabolites to show a significant response, decreasing below the levels in the control plants within 6 h of induction. Martins *et al.* (2013) also observed a tendency for sucrose to decrease in the TPS29.2 plants after induction,

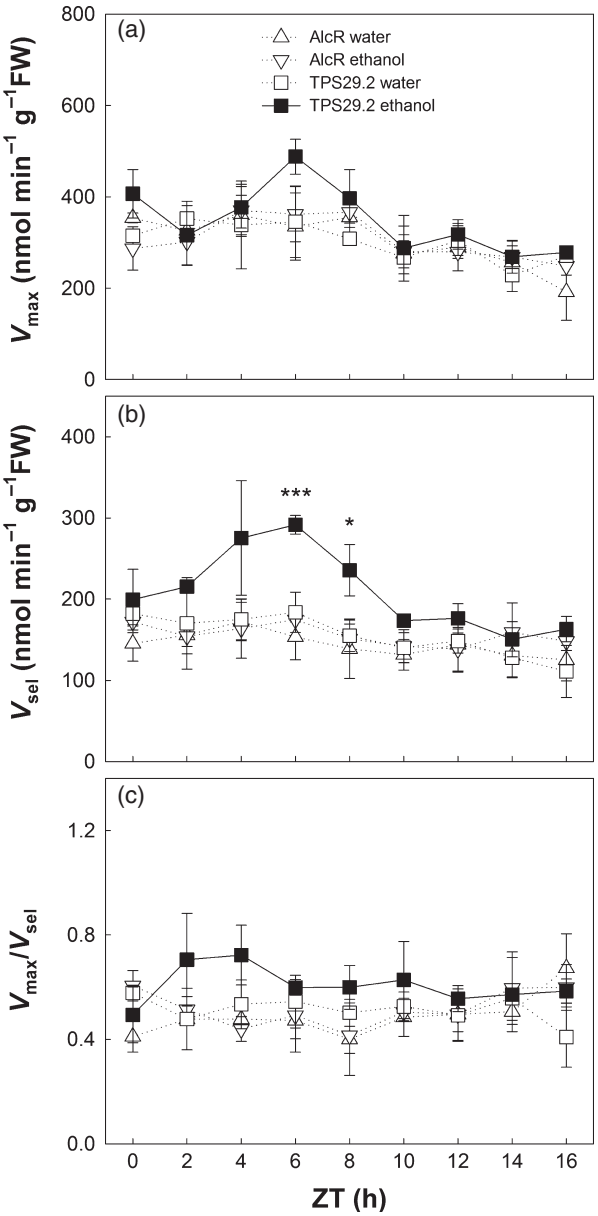


**Figure 5.** TPS induction leads to activation of NR.
Three-week-old TPS29.2 and AlcR plants, grown under long-day conditions (16 h photoperiod), were sprayed with water or 2% v/v ethanol at dawn (ZT0).
(a) NR maximal activity ($V_{max}$).
(b) NR selective activity ($V_{sel}$).
(c) NR activation state ($V_{max}/V_{sel}$).
Values are means ±SD ($n$ = 3). Asterisks indicate statistically significant differences between the induced TPS29.2 and control samples: *$P$ < 0.05, **$P$ < 0.01 and ***$P$ < 0.001 (one-way ANOVA, Holm–Šídák post hoc testing). ZT, Zeitgeber time (hours after dawn).

but their data were more variable and the differences were not statistically significant. This change in sucrose content is consistent with the sucrose–Tre6P nexus model, which predicts that increasing Tre6P will trigger a decrease in sucrose concentration (Yadav *et al.*, 2014). The nexus model was partly based on the low levels of sucrose observed in *35S:otsA* plants. Caution is required when interpreting any of the phenotypic traits of these plants, due to confounding secondary effects when Tre6P levels are permanently elevated. However, our results for the ethanol-inducible otsA line provide compelling evidence that a decrease in sucrose is among the earliest responses to a increase in Tre6P, supporting the concept of Tre6P being a negative feedback regulator of sucrose concentrations. An even more dramatic and rapid decrease of sucrose was observed by Martins *et al.* (2013) after inducing *otsA* expression in the night-time, in this case due to inhibition of starch degradation.

The observed decrease in daytime sucrose levels in the rosettes of induced TPS29.2 plants might be brought about in several different, but not mutually exclusive, ways: (i) decreased synthesis due to lower rates of $CO_2$ assimilation or partitioning into sucrose, (ii) increased export, and (iii) increased consumption by respiration and growth-related processes.

Considering the first possibility, a decrease in the total supply of photoassimilates may be ruled out, as the total amount of carbon in the major metabolite pools (starch, soluble sugars, TCA pathway intermediates and amino acids) was not different or, if anything, was slightly increased in the induced TPS29.2 plants (Figure S4). Furthermore, no differences in $CO_2$ assimilation rates were observed between induced TPS29.2 and control plants when measured directly by gas exchange analysis (Martins *et al.*, 2013). However, the $^{14}$C-labelling data suggested that a smaller proportion of total photoassimilate was partitioned into sucrose in the induced TPS29.2 plants, and more was partitioned into organic acids (Figure S5a,b). Sucrose synthesis is controlled primarily by the cytosolic fructose-1,6–bisphosphatase (FBPase) and SPS (Stitt *et al.*, 1988; Huber *et al.*, 1989). FBPase activity is regulated by Fru2,6BP (Stitt and Heldt, 1985; Stitt *et al.*, 1985), but the levels of this inhibitor were not affected by TPS induction. SPS is subject to allosteric regulation by Glc6P (activator) and Pi (inhibitor), and by multi-site protein phosphorylation mediated by SnRK1 and calcium-dependent protein kinases (CDPKs) (Huber *et al.*, 1989). The decrease in the levels of the product (Suc6P, Figure S1a) is consistent with a decrease in SPS activity. Although the maximal ($V_{max}$) and selective ($V_{sel}$) activities of SPS were unaffected in the induced TPS29.2 plants (Figure S2e), there was a decrease in the content of one of the substrates (Fru6P) and the allosteric activator (Glc6P) (Figure 2, and Figures S1a, S2a and S3). This indicates that sucrose synthesis is decreased due to a decrease in the supply of hexose phosphates. Export of photoassimilates from leaf 4 to the rest of the rosette was not significantly affected in the induced TPS29.2 plants (Figure S5e).

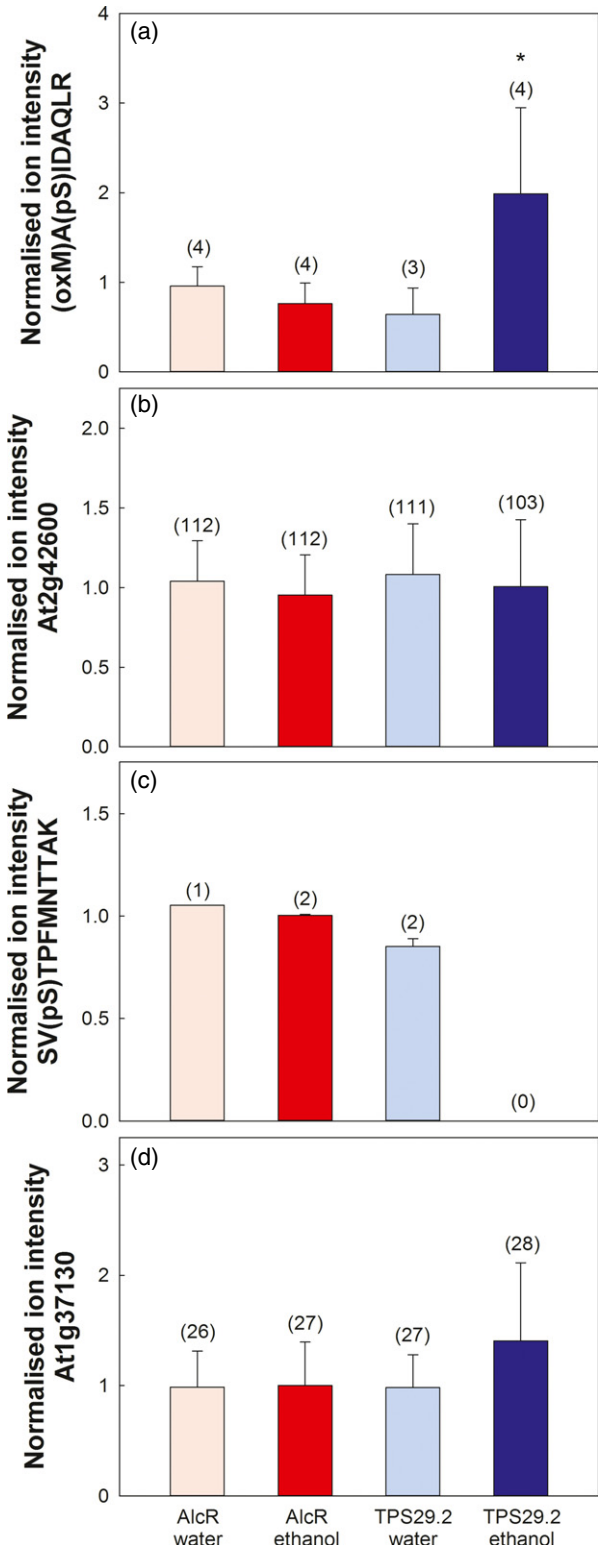


**Figure 6.** TPS induction leads to changes in the phosphorylation of PEPC and NR.
Four-week-old TPS29.2 and AlcR plants, grown under equinoctial conditions (12 h photoperiod) were sprayed with water or 2% v/v ethanol at dawn (ZT0) and harvested at 6 h into the photoperiod (ZT6).
(a) PEPC phosphopeptide (oxM)A(pS$^{11}$)IDAQLR.
(b) Total PEPC peptides (PPC2, At2g42600).
(c) NR phosphopeptide SV(pS$^{534}$)TPFMNTTAK.
(d) Total NR peptides (NIA2, At1g37130).
Values are means ±SD ($n = 4$), and the number of spectra analysed is shown in parentheses. Asterisks indicate statistically significant differences between the induced TPS29.2 and control samples: $*P < 0.05$ (one-way ANOVA, Holm–Šídák *post hoc* testing).

Sucrose levels may also decrease if there is an increase in sucrose catabolism. The slightly higher glucose levels in the induced TPS29.2 plants (Figure 2) may be an indication of increased sucrose catabolism via invertases. No differences in the maximal acid and neutral invertase activities were seen in the induced plants (Figure S2e). However, we cannot exclude the possibility that invertase activities were modulated by other mechanisms (Gao *et al.*, 2014; Lin *et al.*, 2015), or that transport of sucrose across the tonoplast allowed increased hydrolysis by vacuolar invertase. Thus, increased sucrose hydrolysis may contribute to the decrease in sucrose, in combination with decreased rates of synthesis due to a decrease in hexose phosphate levels.

Measurement of starch content and $^{14}CO_2$ labelling revealed only a minor and inconsistent increase in the rate of starch synthesis (see also Martins *et al.*, 2013). In contrast, there was a substantial increase in the partitioning of $^{14}C$ into acidic components, such as organic acids, in the induced TPS29.2 plants (Figure S5b). Further evidence for increased flux to organic acids is provided by the slight decrease in the levels of most phosphorylated intermediates and the increase in the levels of many organic acids (Figures 1 and 2 and Figures S1–S3), and the faster increase in $^{13}C$ enrichment of most organic acids after supplying $^{13}CO_2$ (Figure 3).

Thus, we conclude that diversion of photoassimilates away from sucrose synthesis and into respiratory pathways is the main reason for the decrease in sucrose triggered by increasing Tre6P levels in the induced TPS29.2 plants.

### Tre6P diverts carbon into organic and amino acid metabolism via post-translational activation of PEPC and NR

The classical route for entry of carbon into organic acids is via glycolysis and the TCA pathway. The main product of glycolysis, pyruvate, is imported into the mitochondria, where it is decarboxylated by mitochondrial pyruvate dehydrogenase (mPDH) to give acetyl-CoA, which then enters the TCA pathway as citrate via condensation with OAA by citrate synthase (Figure 2). Oxidation of citrate via the TCA pathway generates NADH, FADH, ATP and $CO_2$. In parallel with the TCA pathway, anaplerotic synthesis of OAA by PEPC in the cytosol provides a supplementary source of dicarboxylates. OAA itself may be imported into the mitochondria, or may first be reduced to malate and

then to fumarate by cytosolic malate dehydrogenase and fumarase, respectively (Pracharoenwattana *et al.*, 2010). Within the mitochondria, imported dicarboxylates feed into the TCA pathway, allowing other intermediates, such as 2–OG, to be withdrawn as carbon skeletons for amino acid synthesis. Although the TCA pathway operates in cyclic flux mode in leaves at night, it operates in illuminated leaves in a linear flux mode with two separate branches, both linked to photorespiratory processes. In one branch, citrate that accumulated during the previous night is converted to 2–OG (Gauthier *et al.*, 2010; Tcherkez *et al.*, 2012), which is necessary to re-assimilate ammonium released by photorespiration, while in a separate branch, OAA is reduced to malate and fumarate, enabling excess reducing equivalents from glycine decarboxylation to be exported out of the mitochondria.

*A. thaliana* has four genes encoding PEPC (*AtPPC1–4*), but only *AtPPC1* and *AtPPC2* are highly expressed in rosettes, and the corresponding isoforms account for the majority of PEPC activity in leaves (Shi *et al.*, 2015). In the induced TPS29.2 plants, we observed a simultaneous increase in phosphorylation and a decrease in mono-ubiquitination of PEPC (Figures 4 and 6a,b). Both of these post-translational modifications enhance PEPC activity by decreasing the enzyme's sensitivity to inhibition by malate, as well as increasing its affinity for its substrate, PEP, and its activator, Glc6P (Uhrig *et al.*, 2008; Gregory *et al.*, 2009; O'Leary *et al.*, 2011a). Our results are consistent with the proposal that these two opposing types of post-translational modification of plant-type PEPC are mutually exclusive (O'Leary *et al.*, 2011b).

The molecular mechanisms linking high Tre6P levels to post-translational activation of PEPC remain to be elucidated. They may involve regulation of PEPC kinase, or more indirect mechanisms. $NH_4^+$ has been implicated as a potential trigger for activation of PEPC in the green alga *Selenastrum minutum*, in which dark carbon fixation via PEPC is linearly related to the $NH_4^+$ assimilation rate (Vanlerberghe *et al.*, 1990). Exogenous supply of $NH_4^+$ to isolated leaf cells of poppy (*Papaver somniferum*) or spinach (*Spinacia oleracea*) rapidly increased incorporation of $^{14}CO_2$ into pyruvate, citrate, malate, 2–OG and closely related amino acids (e.g. Ala, Asp and Gln) at the expense of sucrose synthesis, with no effect on starch accumulation (Paul *et al.*, 1978; Larsen *et al.*, 1981). These metabolic changes were attributed to activation of pyruvate kinase and PEPC, and are strikingly similar to those observed in the induced TPS29.2 plants (Figures 1–3 and Figures S1–S3). In wheat (*Triticum aestivum*), nitrate has been implicated in the activation of PEPC and the diversion of carbon from sucrose to organic acids (Champigny and Foyer, 1992; Champigny *et al.*, 1992; Duff and Chollet, 1995).

There are three main sources of $NH_4^+$ in leaves: (i) photorespiratory release of $NH_4^+$ in the glycine decarboxylase reaction, (ii) delivery of $NH_4^+$ from the roots via the xylem, and (iii) reduction of nitrate. The predominant source of $NH_4^+$ in leaves during the day is thought to be photorespiration. Martins *et al.* (2013) compared net $CO_2$ assimilation rates at different intracellular $CO_2$ partial pressures ($C_i$), but found no significant differences between induced TPS29.2 plants and non-induced or AlcR controls. The absence of any differential response of net assimilation to increasing $C_i$ suggests there are no differences in the rates of photorespiration, and (by implication) no differences in the rates of photorespiratory $NH_4^+$ release. Our plants were fertilized with $NH_4NO_3$, so both $NH_4^+$ and $NO_3^-$ are transported to the leaves in the xylem. $NO_3^-$ is assimilated by reduction to nitrite ($NO_2^-$) in the cytosol by NR, and then reduction of $NO_2^-$ to $NH_4^+$ in the chloroplasts by nitrite reductase (Stitt *et al.*, 2002). We observed a significant increase in the activity of NR measured under selective assay conditions that favour the post-translationally activated (i.e. dephosphorylated) form of the enzyme (Figure 5 and Figure S2e) (Kaiser and Huber, 2001). NR activity is regulated by phosphorylation of a highly conserved Ser residue (Ser534 in *A. thaliana*) and subsequent binding to a 14–3–3 regulatory protein in the presence of $Mg^{2+}$, leading to a complex that has no detectable activity (Su *et al.*, 1996; Kaiser and Huber, 2001). The NR selective activity results were confirmed by analysis of NIA2 (phospho)peptides by mass spectrometry (Figure 6c,d). Plant cells generally contain excess nitrite reductase activity to avoid accumulation of toxic $NO_2^-$. Therefore, activation of NR activity is expected to result in increased $NH_4^+$.

In spinach leaves, NR may be phosphorylated by CDPKs and SnRK1, and thereby inactivated (Bachmann *et al.*, 1995, 1996; Sugden *et al.*, 1999). Both types of protein kinase are inhibited by Glc6P and other sugar phosphates (Bachmann *et al.*, 1995; Toroser *et al.*, 2000; Nunes *et al.*, 2013b). This is unlikely to explain the activation of NR seen after an induced increase in Tre6P, because sugar phosphate levels were decreased. SnRK1 activity is also inhibited by Tre6P (Zhang *et al.*, 2009), apparently offering a simple explanation for the observed decrease in phosphorylation of the NR protein and increase in NR selective activity in induced TPS29.2 plants with high Tre6P levels. However, several considerations argue against this simple scenario. First, NR is located primarily in photosynthetically active (mesophyll) cells in the source leaves, in which SnRK1 is relatively insensitive to Tre6P due to the absence of an unknown protein factor that confers sensitivity to Tre6P inhibition (Zhang *et al.*, 2009). Second, we found no evidence of changes in the activation state of SPS, which, like NR, is also regulated via protein phosphorylation by SnRK1 and CDPKs (Huber *et al.*, 1989). Activation by Tre6P of the protein phosphatase that dephosphorylates the phosphorylated Ser534 residue of NR cannot be excluded as a potential mechanism for the observed activation of NR.

### Tre6P stimulates carbon flux to citrate and 2–oxoglutarate

Together, our $^{13}CO_2$ and $^{14}CO_2$ labelling experiments show that Tre6P has an especially large impact on the flux of photoassimilate to citrate and its immediate derivatives in the TCA pathway (aconitate, isocitrate and 2–OG). The synthesis of citrate via citrate synthase is restricted during the day because mPDH is inhibited in the light (Budde and Randall, 1990; Gemel and Randall, 1992); thus, citrate is mainly produced via this route in the dark (Gauthier *et al.*, 2010; Tcherkez *et al.*, 2012; Ishihara *et al.*, 2015). In the long-day experiment, there was a gradual decrease in citrate levels in the control plants during the day, but a striking increase in citrate levels in the induced TPS29.2 plants (Figure 1e). This was corroborated by the results of the $^{13}CO_2$ labelling experiment, which showed enhanced incorporation of $^{13}C$ into citrate and downstream intermediates in the TCA pathway, i.e. aconitate, isocitrate and 2–OG (Figure 3b–e). This implies that synthesis of acetyl-CoA by mPDH in the light is stimulated by Tre6P. The multiplicity of mitochondrial and plastidial PDH isoforms and the lack of mPDH-specific antibodies hindered the performance of experiments to test the effects of increased Tre6P levels on mPDH activity, but addressing this question is clearly of interest in future investigations.

mPDH is inhibited by its products (acetyl-CoA and NADH) and by protein phosphorylation via a protein kinase that is itself inhibited by pyruvate and activated by $NH_4^+$ (Tovar-Mendez *et al.*, 2003). The activation of PEPC in the induced TPS29.2 plants stimulates flux of $^{13}C$ into malate and fumarate. If malate is transported into the mitochondria, it may be decarboxylated to pyruvate by $NAD^+$-malic enzyme (NAD–ME), providing an alternative source of substrate for mPDH and potentially stimulating mPDH activity by inhibiting mPDH protein kinase (Igamberdiev *et al.*, 2014). Entry of fumarate into the mitochondria may promote this cascade by relieving inhibition of the NAD–ME by malate (Tronconi *et al.*, 2015). Increased flux of organic acids through the mPDH, isocitrate dehydrogenase, 2–OG dehydrogenase and NAD–ME reactions accelerates production of NADH in the mitochondria. However, oxidation of NADH by the mitochondrial electron transport chain to drive oxidative phosphorylation is not needed in the light, as photosynthesis provides all of the ATP needed by the leaf. If there is insufficient capacity to export reducing equivalents from the mitochondria via the OAA/malate shuttle, the mitochondrial NAD(H) pool is likely to become more reduced. This in turn may alter the poise of the glycine decarboxylase reaction, with a higher concentration of glycine being needed in the mitochondria to maintain flux through the glycine decarboxylase reaction. Thus enhanced anaplerotic carbon fixation by PEPC in the induced TPS29.2 plants may explain not only increased synthesis of malate and fumarate (Figure 3g,h), but also the observed increases in citrate, other TCA pathway intermediates and glycine.

In conclusion, induced short-term increases in Tre6P lead to a decrease in sucrose levels, as predicted by the sucrose–Tre6P nexus model. The most likely explanation for the decrease in sucrose is diversion of photoassimilates away from sucrose synthesis towards synthesis of organic and amino acids. Increasing Tre6P levels are associated with activation of NR and PEPC by post-translational modifications, implicating the protein kinases, protein phosphatases and other enzymes (e.g. E3 ligase and deubiquitinating enzyme) involved in these modifications as potential primary targets of Tre6P. Our results also suggest that Tre6P activates flux via mPDH and citrate synthase. Although many of the molecular details remain to be elucidated, our results reveal an important role for Tre6P in coordinating carbon and nitrogen metabolism in plants. It is well known that nitrate and ammonium stimulate the synthesis of organic acids to act as acceptors for the assimilated nitrogen, and that the assimilation of inorganic nitrogen sources is restricted when the carbon supply is low (Stitt *et al.*, 2002; Foyer *et al.*, 2006; Nunes-Nesi *et al.*, 2010). It may be envisaged that Tre6P plays an important role in coordinating the rates of nitrate assimilation and organic acid synthesis with the supply of sucrose.

## EXPERIMENTAL PROCEDURES

### Plant material and growth conditions

Seeds of the *Arabidopsis thaliana* [L.] Heynh. TPS29.2 and AlcR lines were germinated on soil mixed with vermiculite (1:1) as described by Martins *et al.* (2013). After germination, seedlings were transferred to 10 cm diameter pots (four or five seedlings per pot), and grown in a controlled environment chamber (Percival Scientific, http://www.percival-scientific.com) with an irradiance of 150 μmol $m^{-2}$ $sec^{-1}$ and a constant temperature of 20°C, under either a 12 h or 16 h photoperiod. Plants were sprayed with either water or 2% v/v ethanol at the start of the day when they were 3 weeks old (16 h photoperiod) or 4 weeks old (12 h photoperiod). Whole rosettes were harvested in the light and immediately quenched in liquid nitrogen, with four or five plants from the same pot being pooled for each biological replicate. Frozen plant tissue was ground to a fine powder at −70°C in a robotized cryogenic grinder (Labman Automation Ltd, http://www.labman.co.uk) and stored at −80°C until use.

### Metabolite extraction and measurement

Tre6P, phosphorylated intermediates and organic acids were extracted with chloroform/methanol, and measured by high-performance anion-exchange liquid chromatography coupled to tandem mass spectrometry (LC-MS/MS) as described by Lunn *et al.* (2006), with minor modifications (see Methods S1 for further details). Soluble sugars (glucose, fructose and sucrose) were extracted using ethanol and enzymatically assayed as described by Stitt *et al.* (1989). Amino acids were measured in the ethanolic extract by HPLC with fluorescence detection as described by Watanabe *et al.* (2013). Starch was enzymatically determined in the insoluble material remaining after the ethanolic extraction

(Hendriks *et al.*, 2003). Fru2,6BP was extracted using 10 mM KOH as described by Draborg *et al.* (2001), and measured by its activation of potato tuber diphosphate-fructose-6–phosphate 1–phosphotransferase (EC 2.7.1.90; Stitt, 1990b) using a 96-well microplate.

### Enzyme activity assays

Enzymes (NR, acid and neutral invertases, and SPS) were extracted and assayed as described by Gibon *et al.* (2004), with the NR assays based on Kaiser and Brendle-Behnisch (1991). The SPS assay conditions were optimized to distinguish the activated and deactivated forms of the enzyme as described by Trevanion *et al.* (2004). The SPS $V_{max}$ assay mixture contained 6 mM UDPGlc, 6 mM Fru6P and 21 mM Glc6P, while the $V_{sel}$ assay mixture contained 6 mM UDPGlc, 2 mM Fru6P, 7 mM Glc6P and 6 mM $KH_2PO_4$.

### Protein electrophoresis and immunodetection of PEPC

Proteins were extracted using pre-heated sample buffer and immediately subjected to SDS–PAGE in 8% polyacrylamide gels. Proteins were transferred to nitrocellulose membranes and probed using a polyclonal rabbit anti-RcPPC3 antibody for detection of non-ubiquitinated (p107) and mono-ubiquitinated (p110) plant-type PEPC polypeptides (O'Leary *et al.*, 2011a). Phosphorylated plant-type PEPC subunits were detected using a polyclonal rabbit antibody raised against a phospho-Ser11 containing peptide (Gregory *et al.*, 2009). Alternatively, samples were electrophoresed in 7% polyacrylamide gels supplemented with 25 μM Phos-tag acrylamide (Wako Chemicals, http://www.wako-chemicals.de) and 50 μM $MnCl_2$, transferred to nitrocellulose membranes, and probed with anti-RcPPC3 for detection of the phosphorylated PEPC isoform (Gregory *et al.*, 2009). Chromogenic detection was performed using goat anti-rabbit IgG (Fc) conjugated to alkaline phosphatase (Promega, http://www.promega.de). Immunodetections were performed at least twice, and representative results are shown. Band intensities were analysed using the LabImage Platform version 3.2.0 (Kapelan Bio-Imaging, http://www.kapelan-bioimaging.com).

### $^{14}CO_2$ single-leaf labelling

Plants grown under a 16 h photoperiod were used for single-leaf labelling (Kölling *et al.*, 2013). Three-week-old plants were sprayed with either water or 2% v/v ethanol at ZT1, and leaf 4 was supplied with 11.1 MBq $^{14}CO_2$ (specific activity 15.7 MBq mol$^{-1}$) for 5 min at 6 and 12 h after spraying (ZT7 and ZT13, respectively). The pulse was followed by a 1 h chase period at ambient $CO_2$ in the light, and samples were quenched in boiling 80% v/v ethanol for 10 min. Each sample was then separated into three fractions: water-soluble (soluble metabolites), insoluble (starch, proteins and cell wall) and ethanol-soluble (lipids, pigments and waxes). The amount of $^{14}C$ incorporated in each fraction was added to obtain the total $^{14}C$ incorporated into each tissue (leaf 4 or rosette). Single leaves and rosettes were used to estimate the carbon export rate. Partitioning of $^{14}C$ into neutral, acidic and basic components in the water-soluble extract from leaf 4 was determined as described by Kölling *et al.* (2013). A detailed description of these procedures is given in Methods S2.

### $^{13}CO_2$ whole-rosette labelling

Three-week-old plants grown under a 16 h photoperiod were sprayed with either water or 2% v/v ethanol at the start of the day. Four hours after spraying, plants were placed in labelling chambers and supplied with $^{13}CO_2$ (isotopic purity 99 atomic percent; Campro Scientific GmbH) Campro Scientific GmbH, http://www.campro.eu) for 6 h as described by Ishihara *et al.* (2015). Samples were harvested immediately before the start of the pulse and at 2, 4, and 6 h into the labelling period, and isotopomers were measured in chloroform/methanol extracts by LC-MS/MS as described in Methods S3. The isotopomers analysed are listed in Table S3.

### Analysis of peptides and phosphopeptides by mass spectrometry

Samples (100 mg fresh weight) from plants grown under equinoctial conditions and harvested at ZT6 were used for analysis of peptides and phosphopeptides by LC-MS/MS. Protein preparation, phosphopeptide enrichment, LC-MS/MS of peptides and phosphopeptides, mass spectrometric data analysis, and statistical analysis were performed as described by Wu *et al.* (2014). Further details are presented in Methods S4.

### Data analysis and statistics

The number of biological replicates ($n$) in each experiment is indicated in the figure legends. Data from individual time points over the 12 and 16 h time periods were analysed using one-way ANOVA followed by an all, pairwise, multiple comparison procedure (Holm–Šídák method). Differences between the induced TPS29.2 and control plants were considered significant only when the post hoc test showed significant differences ($P < 0.05$) between the induced TPS29.2 samples and each of the controls. The data were also analysed using one-way repeated-measures ANOVA followed by the same post hoc test. All statistical analyses were performed using SigmaPlot 12.5 (Systat Software, http://www.systat.com).

## ACKNOWLEDGEMENTS

The authors thank Christin Abel for technical assistance, and Stéphanie Arrivault, Igor Florez-Sarasa and Martin Lauxmann for advice and helpful discussions. C.M.F. thanks N.M.E. and C.F. for their everyday support. C.M.F. is a researcher from the Argentinian Consejo Nacional de Investigaciones Científicas y Técnicas (CONICET). This work was financed by the Max Planck Society.

## SUPPORTING INFORMATION

Additional Supporting Information may be found in the online version of this article.

**Figure S1.** Changes in metabolites after induction of TPS over-expression under long-day conditions.

**Figure S2.** Changes in metabolites and enzyme activities after induction of TPS over-expression under equinoctial conditions.

**Figure S3.** Overview of metabolite changes after induction of TPS expression.

**Figure S4.** Changes in carbon accumulation after induction of TPS over-expression.

**Figure S5.** Effect of TPS induction on carbon fluxes.

**Figure S6.** Effect of TPS induction on Tre6P and organic acid levels.

**Figure S7.** TPS induction leads to changes in the phosphorylation status of PEPC.

**Figure S8.** Fragmentation spectra for PEPC and NR phosphopeptides.

**Table S1.** Changes in metabolites after induction of TPS over-expression under long-day conditions.

**Table S2.** Changes in metabolites after induction of TPS over-expression under equinoctial conditions.

**Table S3.** Parent and product ions analysed by LC-MS/MS in samples from the $^{13}C$ labelling experiment.

**Methods S1.** Analysis of metabolites by LC-MS/MS.

**Methods S2.** $^{14}CO_2$ single-leaf labelling.

**Methods S3.** $^{13}CO_2$ whole-rosette labelling.

**Methods S4.** Analysis of peptides and phosphopeptides by mass spectrometry.

## REFERENCES


**Bachmann, M., McMichael, R.W. Jr, Huber, J.L., Kaiser, W.M. and Huber, S.C.** (1995) Partial purification and characterization of a calcium-dependent protein kinase and an inhibitor protein required for inactivation of spinach leaf nitrate reductase. *Plant Physiol.*, **108**, 1083–1091.

**Bachmann, M., Shiraishi, N., Campbell, W.H., Yoo, B.C., Harmon, A.C. and Huber, S.C.** (1996) Identification of Ser-543 as the major regulatory phosphorylation site in spinach leaf nitrate reductase. *Plant Cell*, **8**, 505–517.

**Budde, R.J. and Randall, D.D.** (1990) Pea leaf mitochondrial pyruvate dehydrogenase complex is inactivated *in vivo* in a light-dependent manner. *Proc. Natl Acad. Sci. USA*, **87**, 673–676.

**Cabib, E. and Leloir, L.F.** (1958) The biosynthesis of trehalose phosphate. *J. Biol. Chem.*, **231**, 259–275.

**Carillo, P., Feil, R., Gibon, Y., Satoh-Nagasawa, N., Jackson, D., Blasing, O.E., Stitt, M. and Lunn, J.E.** (2013) A fluorometric assay for trehalose in the picomole range. *Plant Methods*, **9**, 21.

**Champigny, M.L. and Foyer, C.** (1992) Nitrate activation of cytosolic protein kinases diverts photosynthetic carbon from sucrose to amino acid biosynthesis: basis for a new concept. *Plant Physiol.*, **100**, 7–12.

**Champigny, M.L., Brauer, M., Bismuth, E., Thi Manh, C., Siegl, G., Van Quy, L. and Stitt, M.** (1992) The short-term effect of $NO_3^-$ and $NH_3$ assimilation on sucrose synthesis in leaves. *J. Plant Physiol.*, **139**, 361–368.

**Debast, S., Nunes-Nesi, A., Hajirezaei, M.R., Hofmann, J., Sonnewald, U., Fernie, A.R. and Bornke, F.** (2011) Altering trehalose-6–phosphate content in transgenic potato tubers affects tuber growth and alters responsiveness to hormones during sprouting. *Plant Physiol.*, **156**, 1754–1771.

**Delorge, I., Figueroa, C.M., Feil, R., Lunn, J.E. and Van Dijck, P.** (2015) Trehalose-6–phosphate synthase 1 is not the only active TPS in *Arabidopsis thaliana*. *Biochem J.*, **466**, 283–290.

**van Dijken, A.J., Schluepmann, H. and Smeekens, S.C.** (2004) *Arabidopsis* trehalose-6–phosphate synthase 1 is essential for normal vegetative growth and transition to flowering. *Plant Physiol.*, **135**, 969–977.

**Draborg, H., Villadsen, D. and Nielsen, T.H.** (2001) Transgenic *Arabidopsis* plants with decreased activity of fructose-6–phosphate,2–kinase/fructose-2,6–bisphosphatase have altered carbon partitioning. *Plant Physiol.*, **126**, 750–758.

**Duff, S. and Chollet, R.** (1995) *In vivo* regulation of wheat-leaf phospho*enol*pyruvate carboxylase by reversible phosphorylation. *Plant Physiol.*, **107**, 775–782.

**Eastmond, P.J., van Dijken, A.J., Spielman, M., Kerr, A., Tissier, A.F., Dickinson, H.G., Jones, J.D., Smeekens, S.C. and Graham, I.A.** (2002) Trehalose-6–phosphate synthase 1, which catalyses the first step in trehalose synthesis, is essential for *Arabidopsis* embryo maturation. *Plant J.*, **29**, 225–235.

**Foyer, C.H., Noctor, G. and Verrier, P.** (2006) Photosynthetic carbon–nitrogen interactions: modelling inter-pathway control and signalling. In *Annual Plant Reviews, Volume 22: control of Primary Metabolism in Plants* (Plaxton, W.C. and McManus, M.T., eds). Oxford: Blackwell, pp. 325–347.

**Gao, J., van Kleeff, P.J., Oecking, C., Li, K.W., Erban, A., Kopka, J., Hincha, D.K. and de Boer, A.H.** (2014) Light-modulated activity of root alkaline/neutral invertase involves the interaction with 14–3–3 proteins. *Plant J.*, **80**, 785–796.

**Gauthier, P.P., Bligny, R., Gout, E., Mahe, A., Nogues, S., Hodges, M. and Tcherkez, G.G.** (2010) *In folio* isotopic tracing demonstrates that nitrogen assimilation into glutamate is mostly independent from current $CO_2$ assimilation in illuminated leaves of *Brassica napus*. *New Phytol.*, **185**, 988–999.

**Gemel, J. and Randall, D.D.** (1992) Light regulation of leaf mitochondrial pyruvate dehydrogenase complex: role of photorespiratory carbon metabolism. *Plant Physiol.*, **100**, 908–914.

**Gibon, Y., Blaesing, O.E., Hannemann, J., Carillo, P., Hohne, M., Hendriks, J.H., Palacios, N., Cross, J., Selbig, J. and Stitt, M.** (2004) A robot-based platform to measure multiple enzyme activities in *Arabidopsis* using a set of cycling assays: comparison of changes of enzyme activities and transcript levels during diurnal cycles and in prolonged darkness. *Plant Cell*, **16**, 3304–3325.

**Gomez, L.D., Baud, S., Gilday, A., Li, Y. and Graham, I.A.** (2006) Delayed embryo development in the *Arabidopsis trehalose-6–phosphate synthase 1* mutant is associated with altered cell wall structure, decreased cell division and starch accumulation. *Plant J.*, **46**, 69–84.

**Gomez, L.D., Gilday, A., Feil, R., Lunn, J.E. and Graham, I.A.** (2010) AtTPS1-mediated trehalose 6–phosphate synthesis is essential for embryogenic and vegetative growth and responsiveness to ABA in germinating seeds and stomatal guard cells. *Plant J.*, **64**, 1–13.

**Gregory, A.L., Hurley, B.A., Tran, H.T., Valentine, A.J., She, Y.M., Knowles, V.L. and Plaxton, W.C.** (2009) *In vivo* regulatory phosphorylation of the phosphoenolpyruvate carboxylase AtPPC1 in phosphate-starved *Arabidopsis thaliana*. *Biochem J.*, **420**, 57–65.

**Hartwell, J., Gill, A., Nimmo, G.A., Wilkins, M.B., Jenkins, G.I. and Nimmo, H.G.** (1999) Phosphoenolpyruvate carboxylase kinase is a novel protein kinase regulated at the level of expression. *Plant J.*, **20**, 333–342.

**Hendriks, J.H., Kolbe, A., Gibon, Y., Stitt, M. and Geigenberger, P.** (2003) ADP-glucose pyrophosphorylase is activated by posttranslational redox modification in response to light and to sugars in leaves of *Arabidopsis* and other plant species. *Plant Physiol.*, **133**, 838–849.

**Huber, J.L., Huber, S.C. and Nielsen, T.H.** (1989) Protein phosphorylation as a mechanism for regulation of spinach leaf sucrose-phosphate synthase activity. *Arch. Biochem. Biophys.*, **270**, 681–690.

**Igamberdiev, A.U., Lernmark, U. and Gardestrom, P.** (2014) Activity of the mitochondrial pyruvate dehydrogenase complex in plants is stimulated in the presence of malate. *Mitochondrion*, **19**, 184–190.

**Ishihara, H., Obata, T., Sulpice, R., Fernie, A.R. and Stitt, M.** (2015) Quantifying protein synthesis and degradation in arabidopsis by dynamic $^{13}CO_2$ labeling and analysis of enrichment in individual amino acids in their free pools and in protein. *Plant Physiol.*, **168**, 74–93.

**Kaiser, W.M. and Brendle-Behnisch, E.** (1991) Rapid modulation of spinach leaf nitrate reductase activity by photosynthesis: I. Modulation *in vivo* by $CO_2$ availability. *Plant Physiol.*, **96**, 363–367.

**Kaiser, W.M. and Huber, S.C.** (2001) Post-translational regulation of nitrate reductase: mechanism, physiological relevance and environmental triggers. *J. Exp. Bot.*, **52**, 1981–1989.

**Kinoshita, E., Kinoshita-Kikuta, E., Takiyama, K. and Koike, T.** (2006) Phosphate-binding tag, a new tool to visualize phosphorylated proteins. *Mol. Cell Proteomics*, **5**, 749–757.

**Kölling, K., Müller, A., Flütsch, P. and Zeeman, S.C.** (2013) A device for single leaf labelling with $CO_2$ isotopes to study carbon allocation and partitioning in *Arabidopsis thaliana*. *Plant Methods*, **9**, 45.

**Larsen, P.O., Cornwell, K.L., Gee, S.L. and Bassham, J.A.** (1981) Amino acid synthesis in photosynthesizing spinach cells: effects of ammonia on pool sizes and rates of labeling from $CO_2$. *Plant Physiol.*, **68**, 292–299.

**Lastdrager, J., Hanson, J. and Smeekens, S.** (2014) Sugar signals and the control of plant growth and development. *J. Exp. Bot.*, **65**, 799–807.

**Lin, Y., Liu, T., Liu, J., Liu, X., Ou, Y., Zhang, H., Li, M., Sonnewald, U., Song, B. and Xie, C.** (2015) Subtle regulation of potato acid invertase activity by a protein complex of invertase, invertase inhibitor, and SUCROSE NONFERMENTING1-RELATED PROTEIN KINASE. *Plant Physiol.*, **168**, 1807–1819.

**Lunn, J.E.** (2008) Sucrose metabolism. In *Encyclopedia of Life Sciences* (Roberts, K., ed). Chichester, UK: Wiley, www.els.net. doi: 10.1002/97804700
15902.a0021259.

**Lunn, J.E., Feil, R., Hendriks, J.H., Gibon, Y., Morcuende, R., Osuna, D., Scheible, W.R., Carillo, P., Hajirezaei, M.R. and Stitt, M.** (2006) Sugar-induced increases in trehalose 6–phosphate are correlated with redox activation of ADP-glucose pyrophosphorylase and higher rates of starch synthesis in *Arabidopsis thaliana*. *Biochem J.*, **397**, 139–148.

**Lunn, J.E., Delorge, I., Figueroa, C.M., Van Dijck, P. and Stitt, M.** (2014) Trehalose metabolism in plants. *Plant J.*, **79**, 544–567.

**Martinez-Barajas, E., Delatte, T., Schluepmann, H., de Jong, G.J., Somsen, G.W., Nunes, C., Primavesi, L.F., Coello, P., Mitchell, R.A. and Paul, M.J.**

(2011) Wheat grain development is characterized by remarkable trehalose 6–phosphate accumulation pregrain filling: tissue distribution and relationship to SNF1-related protein kinase1 activity. *Plant Physiol.*, **156**, 373–381.

**Martins, M.C., Hejazi, M., Fettke, J. *et al.*** (2013) Feedback inhibition of starch degradation in *Arabidopsis* leaves mediated by trehalose 6–phosphate. *Plant Physiol.*, **163**, 1142–1163.

**Nunes, C., O'Hara, L.E., Primavesi, L.F., Delatte, T.L., Schluepmann, H., Somsen, G.W., Silva, A.B., Fevereiro, P.S., Wingler, A. and Paul, M.J.** (2013a) The trehalose 6–phosphate/SnRK1 signaling pathway primes growth recovery following relief of sink limitation. *Plant Physiol.*, **162**, 1720–1732.

**Nunes, C., Primavesi, L.F., Patel, M.K., Martinez-Barajas, E., Powers, S.J., Sagar, R., Fevereiro, P.S., Davis, B.G. and Paul, M.J.** (2013b) Inhibition of SnRK1 by metabolites: tissue-dependent effects and cooperative inhibition by glucose 1–phosphate in combination with trehalose 6–phosphate. *Plant Physiol. Biochem.*, **63**, 89–98.

**Nunes-Nesi, A., Fernie, A.R. and Stitt, M.** (2010) Metabolic and signaling aspects underpinning the regulation of plant carbon nitrogen interactions. *Mol. Plant*, **3**, 973–996.

**O'Leary, B., Fedosejevs, E.T., Hill, A.T., Bettridge, J., Park, J., Rao, S.K., Leach, C.A. and Plaxton, W.C.** (2011a) Tissue-specific expression and post-translational modifications of plant- and bacterial-type phosphoenolpyruvate carboxylase isozymes of the castor oil plant, *Ricinus communis* L. *J. Exp. Bot.*, **62**, 5485–5495.

**O'Leary, B., Park, J. and Plaxton, W.C.** (2011b) The remarkable diversity of plant PEPC (phosphoenolpyruvate carboxylase): recent insights into the physiological functions and post-translational controls of non-photosynthetic PEPCs. *Biochem J.*, **436**, 15–34.

**Paul, J.S., Cornwell, K.L. and Bassham, J.A.** (1978) Effects of ammonia on carbon metabolism in photosynthesizing isolated mesophyll cells from *Papaver somniferum* L. *Planta*, **142**, 49–54.

**Plaxton, W.C. and Podestá, F.E.** (2006) The functional organization and control of plant respiration. *Crit. Rev. Plant Sci.*, **25**, 159–198.

**Pracharoenwattana, I., Zhou, W., Keech, O., Francisco, P.B., Udomchalothorn, T., Tschoep, H., Stitt, M., Gibon, Y. and Smith, S.M.** (2010) *Arabidopsis* has a cytosolic fumarase required for the massive allocation of photosynthate into fumaric acid and for rapid plant growth on high nitrogen. *Plant J.*, **62**, 785–795.

**Ruiz-Ballesta, I., Feria, A.B., Ni, H., She, Y.M., Plaxton, W.C. and Echevarria, C.** (2014) *In vivo* monoubiquitination of anaplerotic phosphoenolpyruvate carboxylase occurs at Lys624 in germinating sorghum seeds. *J. Exp. Bot.*, **65**, 443–451.

**Schluepmann, H., Pellny, T., van Dijken, A., Smeekens, S. and Paul, M.** (2003) Trehalose 6–phosphate is indispensable for carbohydrate utilization and growth in *Arabidopsis thaliana*. *Proc. Natl Acad. Sci. USA*, **100**, 6849–6854.

**Shane, M.W., Fedosejevs, E.T. and Plaxton, W.C.** (2013) Reciprocal control of anaplerotic phosphoenolpyruvate carboxylase by *in vivo* monoubiquitination and phosphorylation in developing proteoid roots of phosphate-deficient harsh hakea. *Plant Physiol.*, **161**, 1634–1644.

**Shi, J., Yi, K., Liu, Y. *et al.*** (2015) Phospho*enol*pyruvate carboxylase in *Arabidopsis* leaves plays a crucial role in carbon and nitrogen metabolism. *Plant Physiol.*, **167**, 671–681.

**Stitt, M.** (1990a) Fructose-2,6–bisphosphate as a regulatory molecule in plants. *Annu. Rev. Plant Physiol. Plant Mol. Biol.*, **41**, 153–185.

**Stitt, M.** (1990b) Fructose 2,6–bisphosphate. In *Methods in Plant Biochemistry* (Lea, P.J., ed.). London: Academic Press, pp. 87–92.

**Stitt, M. and Heldt, H.W.** (1985) Control of photosynthetic sucrose synthesis by fructose 2,6–bisphosphate: VI. Regulation of the cytosolic fructose 1,6–bisphosphatase in spinach leaves by an interaction between metabolic intermediates and fructose 2,6–bisphosphate. *Plant Physiol.*, **79**, 599–608.

**Stitt, M., Herzog, B. and Heldt, H.W.** (1985) Control of photosynthetic sucrose synthesis by fructose 2,6–bisphosphate: V. Modulation of the spinach leaf cytosolic fructose 1,6–bisphosphatase activity *in vitro* by substrate, products, pH, magnesium, fructose 2,6–bisphosphate, adenosine monophosphate, and dihydroxyacetone phosphate. *Plant Physiol.*, **79**, 590–598.

**Stitt, M., Wilke, I., Feil, R. and Heldt, H.W.** (1988) Coarse control of sucrose-phosphate synthase in leaves: alterations of the kinetic properties in response to the rate of photosynthesis and the accumulation of sucrose. *Planta*, **174**, 217–230.

**Stitt, M., Lilley, R.M., Gerhardt, R. and Heldt, H.W.** (1989) Metabolite levels in specific cells and subcellular compartments of plant leaves. *Methods Enzymol.*, **174**, 518–552.

**Stitt, M., Muller, C., Matt, P., Gibon, Y., Carillo, P., Morcuende, R., Scheible, W.R. and Krapp, A.** (2002) Steps towards an integrated view of nitrogen metabolism. *J. Exp. Bot.*, **53**, 959–970.

**Su, W., Huber, S.C. and Crawford, N.M.** (1996) Identification *in vitro* of a post-translational regulatory site in the hinge 1 region of *Arabidopsis* nitrate reductase. *Plant Cell*, **8**, 519–527.

**Sugden, C., Donaghy, P.G., Halford, N.G. and Hardie, D.G.** (1999) Two SNF1-related protein kinases from spinach leaf phosphorylate and inactivate 3–hydroxy-3–methylglutaryl coenzyme A reductase, nitrate reductase, and sucrose phosphate synthase *in vitro*. *Plant Physiol.*, **120**, 257–274.

**Sulpice, R., Flis, A., Ivakov, A.A., Apelt, F., Krohn, N., Encke, B., Abel, C., Feil, R., Lunn, J.E. and Stitt, M.** (2014) Arabidopsis coordinates the diurnal regulation of carbon allocation and growth across a wide range of photoperiods. *Mol. Plant*, **7**, 137–155.

**Szecowka, M., Heise, R., Tohge, T. *et al.*** (2013) Metabolic fluxes in an illuminated *Arabidopsis* rosette. *Plant Cell*, **25**, 694–714.

**Tcherkez, G., Mahe, A., Guerard, F., Boex-Fontvieille, E.R., Gout, E., Lamothe, M., Barbour, M.M. and Bligny, R.** (2012) Short-term effects of $CO_2$ and $O_2$ on citrate metabolism in illuminated leaves. *Plant, Cell Environ.*, **35**, 2208–2220.

**Toroser, D., Plaut, Z. and Huber, S.C.** (2000) Regulation of a plant SNF1-related protein kinase by glucose-6–phosphate. *Plant Physiol.*, **123**, 403–412.

**Tovar-Mendez, A., Miernyk, J.A. and Randall, D.D.** (2003) Regulation of pyruvate dehydrogenase complex activity in plant cells. *Eur. J. Biochem.*, **270**, 1043–1049.

**Trevanion, S.J., Castleden, C.K., Foyer, C.H., Furbank, R.T., Quick, W.P. and Lunn, J.E.** (2004) Regulation of sucrose-phosphate synthase in wheat (*Triticum aestivum*) leaves. *Funct. Plant Biol.*, **31**, 685–695.

**Tronconi, M.A., Wheeler, M.C., Martinatto, A., Zubimendi, J.P., Andreo, C.S. and Drincovich, M.F.** (2015) Allosteric substrate inhibition of *Arabidopsis* NAD-dependent malic enzyme 1 is released by fumarate. *Phytochemistry*, **111**, 37–47.

**Uhrig, R.G., She, Y.M., Leach, C.A. and Plaxton, W.C.** (2008) Regulatory monoubiquitination of phosphoenolpyruvate carboxylase in germinating castor oil seeds. *J. Biol. Chem.*, **283**, 29650–29657.

**Vanlerberghe, G.C., Schuller, K.A., Smith, R.G., Feil, R., Plaxton, W.C. and Turpin, D.H.** (1990) Relationship between $NH_4^+$ assimilation rate and *in vivo* phospho*enol*pyruvate carboxylase activity. Regulation of anaplerotic carbon flow in the green alga *Selenastrum minutum*. *Plant Physiol.*, **94**, 284–290.

**Wahl, V., Ponnu, J., Schlereth, A., Arrivault, S., Langenecker, T., Franke, A., Feil, R., Lunn, J.E., Stitt, M. and Schmid, M.** (2013) Regulation of flowering by trehalose-6–phosphate signaling in *Arabidopsis thaliana*. *Science*, **339**, 704–707.

**Watanabe, M., Balazadeh, S., Tohge, T., Erban, A., Giavalisco, P., Kopka, J., Mueller-Roeber, B., Fernie, A.R. and Hoefgen, R.** (2013) Comprehensive dissection of spatiotemporal metabolic shifts in primary, secondary, and lipid metabolism during developmental senescence in *Arabidopsis*. *Plant Physiol.*, **162**, 1290–1310.

**Wilkinson, J.Q. and Crawford, N.M.** (1991) Identification of the *Arabidopsis CHL3* gene as the nitrate reductase structural gene *NIA2*. *Plant Cell*, **3**, 461–471.

**Wingler, A., Delatte, T.L., O'Hara, L.E., Primavesi, L.F., Jhurreea, D., Paul, M.J. and Schluepmann, H.** (2012) Trehalose 6–phosphate is required for the onset of leaf senescence associated with high carbon availability. *Plant Physiol.*, **158**, 1241–1251.

**Wu, X., Sklodowski, K., Encke, B. and Schulze, W.X.** (2014) A kinase–phosphatase signaling module with BSK8 and BSL2 involved in regulation of sucrose-phosphate synthase. *J. Proteome Res.*, **13**, 3397–3409.

**Yadav, U.P., Ivakov, A., Feil, R. *et al.*** (2014) The sucrose-trehalose 6–phosphate (Tre6P) nexus: specificity and mechanisms of sucrose signalling by Tre6P. *J. Exp. Bot.*, **65**, 1051–1068.

**Zhang, Y., Primavesi, L.F., Jhurreea, D., Andralojc, P.J., Mitchell, R.A., Powers, S.J., Schluepmann, H., Delatte, T., Wingler, A. and Paul, M.J.** (2009) Inhibition of SNF1-related protein kinase1 activity and regulation of metabolic pathways by trehalose-6–phosphate. *Plant Physiol.*, **149**, 1860–1871.

 